*Inorg. Chem.* **1989**, *28*, 3696-3701

Contribution from the Department of Chemistry, University of Minnesota, Minneapolis, Minnesota 55455, and Department of Inorganic Chemistry, University of Nijmegen, Toernooiveld, 6525 ED Nijmegen, The Netherlands

# Heterobimetallic Au–Pt Phosphine Complexes. X-ray Crystal and Molecular Structures of $[(PPh_3)Pt(AuPPh_3)_6](NO_3)_2$ and $[(PPh_3)(CO)Pt(AuPPh_3)_6](PF_6)_2$

Larry N. Ito,[†] James D. Sweet,[†] Ann M. Mueting,[†] Louis H. Pignolet,[*,†] M. F. J. Schoondergang,[‡] and J. J. Steggerda[‡]

*Received March 21, 1989*

Several new heterobimetallic phosphine complexes containing gold have been synthesized. $[(PPh_3)Pt(AuPPh_3)_6]^{2+}$ (**1**) was made by the reaction of $[(PPh_3)_2(NO_3)Pt(AuPPh_3)_2]^+$ and $H_2$ with $CH_2Cl_2$ as solvent. The reaction of the $NO_3^-$ and $PF_6^-$ salts of **1** with CO, with $CH_2Cl_2$ as solvent, formed $[(PPh_3)(CO)Pt(AuPPh_3)_6]^{2+}$ (**2**), whereas the $Cl^-$ salt of **1** formed $[(PPh_3)(CO)Pt(AuPPh_3)_5]^+$ (**3**), under similar reaction conditions. The $NO_3^-$ and $PF_6^-$ salts of **2** reacted with $PPh_3$ under 1 atm of CO to produce **3**. Complex **3** reacted with $Au(PPh_3)NO_3$ to regenerate **2**. Complexes **1**$(NO_3)_2$ and **2**$(PF_6)_2$ were characterized by single-crystal X-ray diffraction in the solid state [**1**$(NO_3)_2\cdot Et_2O$, triclinic $P\bar{1}$, $a$ = 14.158 (19) Å, $b$ = 16.486 (22) Å, $c$ = 27.091 (23) Å, $\alpha$ = 94.92 (9)°, $\beta$ = 89.84 (9)°, $\gamma$ = 101.23 (11)°, $T$ = −90 °C, $Z$ = 2, $R$ = 0.053 for 9305 observations; **2**$(PF_6)_2$, triclinic $P\bar{1}$, $a$ = 14.33 (1) Å, $b$ = 16.80 (2) Å, $c$ = 28.20 (3) Å, $\alpha$ = 87.84 (9)°, $\beta$ = 82.47 (8)°, $\gamma$ = 66.96 (6)°, $T$ = −84 °C, $Z$ = 2, $R$ = 0.088 for 8466 observations] and by FABMS, IR spectroscopy, and $^{31}P$ and $^{13}C$ NMR spectroscopies in solution. The structure of **1** consists of six $Au(PPh_3)$ units bonded to a $Pt(PPh_3)$ moiety, forming a structure in which the Pt atom and four of the Au atoms form a trigonal bipyramid sharing an edge with a tetrahedron formed by the Pt atom and three of the Au atoms. The average Au–Pt and Au–Au distances in **1** are 2.678 (1) and 2.849 (1) Å, respectively. The structure of **2** is very similar to that of **1**, with the CO ligand bonded to the Pt atom and with one additional Au–Au bonding interaction. The average Au–Pt and Au–Au distances in **2** are 2.687 (1) and 2.896 (1) Å, respectively. Compound **3** was characterized by FABMS and by $^{31}P$ and $^{13}C$ NMR and IR spectroscopies.

## Introduction

The synthesis, structural characterization, and reactivity studies of mixed transition-metal–gold cluster compounds is a rapidly expanding field of study.[1–37] These compounds are important not only because of their novel structural properties and their potential for assisting in understanding the role of gold in bimetallic surface catalysis,[38–41] but also because of their potential as homogeneous bimetallic catalysts. Of the cluster compounds synthesized to date, however, only a few have shown catalytic behavior under homogeneous conditions.[3,39,42–45] It is our goal to continue in the study of new transition-metal–gold cluster compounds, especially ones that contain catalytically important metals such as Pt and Pd, in an effort to develop a better understanding of the role of gold in catalysis.

A variety of transition-metal–gold–phosphine cluster compounds have been prepared in our laboratories,[1–9] including the gold–platinum complex $[(PPh_3)Pt(AuPPh_3)_6]^{2+}$.[5] Exposure of a $CH_2Cl_2$ solution of $[(PPh_3)_2(NO_3)Pt(AuPPh_3)_2]^+$ to 1 atm of $H_2$ resulted in the formation of $[(PPh_3)Pt(AuPPh_3)_6]^{2+}$ (**1**), which was isolated as the $BPh_4^-$ salt.[5] This $Au_6Pt$ complex was also identified as a product of the reaction of $Pt(PPh_3)_3$ with 6 equiv of $Au(PPh_3)NO_3$ under an atmosphere of $H_2$, which has been previously reported to yield $[(PPh_3)(H)Pt(AuPPh_3)_7](NO_3)_2$ and $[Pt(AuPPh_3)_8](NO_3)_2$.[6,8] $[(PPh_3)Pt(AuPPh_3)_6](BPh_4)_2$ (**1**$(BPh_4)_2$) was characterized by $^{31}P$ NMR spectroscopy and FABMS. We have recently carried out a single-crystal X-ray crystallographic analysis of $[(PPh_3)Pt(AuPPh_3)_6](NO_3)_2$ (**1**$(NO_3)_2$), which we report here. The complexes $[(PPh_3)(CO)Pt(AuPPh_3)_6]^{2+}$ (**2**) and $[(PPh_3)(CO)Pt(AuPPh_3)_5]^+$ (**3**) were also synthesized and characterized by spectroscopic methods. Complex **2**$(PF_6)_2$ was further characterized by single-crystal X-ray crystallographic analysis.

## Experimental Section

**Physical Measurements and Reagents.** $^{31}P$ NMR spectra were recorded at 121.5 MHz with use of a Nicolet NT-300 spectrometer, and $^{13}C$ NMR spectra were recorded at 75.5 MHz with use of an IBM AC-300 spectrometer. Both were run with proton decoupling, and $^{31}P$ NMR spectra are reported in ppm relative to internal standard trimethyl phosphate (TMP), with positive shifts downfield. $^{13}C$ NMR spectra are reported in ppm relative to external standard tetramethylsilane (TMS), with positive shifts downfield. Infrared spectra were recorded on a Perkin-Elmer 1710 FT-IR spectrometer. Conductivity measurements were made with use of a Yellow Springs Model 31 conductivity bridge. Compound concentrations used in the conductivity experiments were 3 × $10^{-4}$ M in $CH_3CN$. FABMS experiments were carried out with use

---

[†] University of Minnesota.

[‡] University of Nijmegen.

(1) Mueting, A. M.; Bos, W.; Alexander, B. D.; Boyle, P. D.; Casalnuovo, J. A.; Balaban, S.; Ito, L. N.; Johnson, S. M.; Pignolet, L. H. In "Recent Advances in Di- and Polynuclear Chemistry"; Braunstein, P., Ed. *New J. Chem.* **1988**, *12*, 505 and references cited therein.

(2) Boyle, P. D.; Boyd, D. C.; Mueting, A. M.; Pignolet, L. H. *Inorg. Chem.* **1988**, *27*, 4424.

(3) Alexander, B. D.; Gomez-Sal, M. P.; Gannon, P. R.; Blaine, C. A.; Boyle, P. D.; Mueting, A. M.; Pignolet, L. H. *Inorg. Chem.* **1988**, *27*, 3301.

(4) Bos, W.; Steggerda, J. J.; Shiping, Y.; Casalnuovo, J. A.; Mueting, A. M.; Pignolet, L. H. *Inorg. Chem.* **1988**, *27*, 948.

(5) Boyle, P. D.; Johnson, B. J.; Alexander, B. D.; Casalnuovo, J. A.; Gannon, P. R.; Johnson, S. M.; Larka, E. A.; Mueting, A. M.; Pignolet, L. H. *Inorg. Chem.* **1987**, *26*, 1346.

(6) Kanters, R. P. F.; Bour, J. J.; Schlebos, P. P. J.; Bosman, W. P.; Behm, H.; Steggerda, J. J.; Ito, L. N.; Pignolet, L. H. *Inorg. Chem.* **1989**, *28*, 2591.

(7) Kanters, R. P. F.; Schlebos, P. P. J.; Bour, J. J.; Bosman, W. P.; Behm, H. J.; Steggerda, J. J. *Inorg. Chem.* **1988**, *27*, 4034.

(8) Bour, J. J.; Kanters, R. P. F.; Schlebos, P. P. J.; Steggerda, J. J. *Recl. Trav. Chim. Pays-Bas* **1988**, *107*, 211.

(9) Bour, J. J.; Kanters, R. P. F.; Schlebos, P. P. J.; Bos, W.; Bosman, W. P.; Behm, H.; Beurskens, P. T.; Steggerda, J. J. *J. Organomet. Chem.* **1987**, *329*, 405.

(10) Jones, P. G. *Gold Bull.* **1986**, *19*, 46 and references cited therein.

(11) Braunstein, P.; Rosé, J. *Gold Bull.* **1985**, *18*, 17.

(12) Hall, K. P.; Mingos, D. M. P. *Prog. Inorg. Chem.* **1984**, *32*, 327 and references cited therein.

(13) Mingos, D. M. P.; Oster, P.; Sherman, D. J. *J. Organomet. Chem.* **1987**, *320*, 257.

(14) Gilmour, D. I.; Mingos, D. M. P. *J. Organomet. Chem.* **1986**, *302*, 127.

(15) Hallam, M. F.; Mingos, D. M. P.; Adatia, T.; McPartlin, M. *J. Chem. Soc., Dalton Trans.* **1988**, 335.

(16) Parish, R. V.; Moore, L. S.; Dens, A. J. D.; Mingos, D. M. P.; Sherman, D. J. *J. Chem. Soc., Dalton Trans.* **1988**, 781.

(17) Braunstein, P.; Lehner, H.; Matt, D.; Tiripicchio, A.; Tiripicchio-Camellini, M. *Angew. Chem., Int. Ed. Engl.* **1984**, *23*, 304.

(18) Smith, E. W.; Welch, A. J.; Treurnicht, I.; Puddephatt, R. J. *Inorg. Chem.* **1986**, *25*, 4616.

(19) Manojlović-Muir, L.; Muir, K. W.; Treurnicht, I.; Puddephatt, R. J. *Inorg. Chem.* **1987**, *26*, 2418.

(20) Albinato, A.; Lehner, H.; Venanzi, L. M.; Wolfer, M. *Inorg. Chem.* **1987**, *26*, 3933.

(21) Murray, H. H.; Briggs, D. A.; Garzón, G.; Raptis, R. G.; Porter, L. C.; Fackler, J. P., Jr. *Organometallics* **1987**, *6*, 1992.

(22) Carr, S. W.; Pringle, P. G.; Shaw, B. L. *J. Organomet. Chem.* **1988**, *341*, 543.

(23) Brown, S. S. D.; Salter, I. D.; Dyson, D. B.; Parish, R. V.; Bates, P. A.; Hursthouse, M. B. *J. Chem. Soc., Dalton Trans.* **1988**, 1795.

(24) Adatia, T.; McPartlin, M.; Salter, I. D. *J. Chem. Soc., Dalton Trans.* **1988**, 751.

(25) Moehring, G. A.; Walton, R. A. *J. Chem. Soc., Dalton Trans.* **1988**, 1701.

0020-1669/89/1328-3696$01.50/0

of a VG Analytical, Ltd., 7070E-HF high-resolution double-focusing mass spectrometer equipped with a VG 11/250 data system.[5] Microanalyses were carried out by Analytische Laboratorien, Engelskirchen, West Germany. Solvents were dried and distilled prior to use. $[(PPh_3)_2(NO_3)Pt(AuPPh_3)_2]NO_3$[5] was prepared as described in the literature. All manipulations were carried out under a purified $N_2$ atmosphere with use of standard Schlenk techniques unless otherwise noted.

**Preparation of Compounds. $\mathbf{[(PPh_3)Pt(AuPPh_3)_6](NO_3)_2}$ ($\mathbf{1(NO_3)_2}$)** was prepared by dissolving $[(PPh_3)_2(NO_3)Pt(AuPPh_3)_2]NO_3$ (100 mg, $5.67 \times 10^{-2}$ mmol) in 10 mL in dichloromethane and placing the mixture under 1 atm of $H_2$. The solution was stirred for about 1 h, during which time the color changed from yellow to dark orange-brown. Diethyl ether (60 mL) was added to precipitate a brown material. This product was collected on a fritted filter, washed with 40 mL of diethyl ether, and dried under vacuum. Dark brown X-ray-quality crystals were obtained in the following manner: 50 mg of the brown powder was dissolved in approximately 2 mL of methanol, and this solution was filtered; small portions of diethyl ether were added, with mixing after each addition, until the solution became slightly cloudy (approximately 15 mL of diethyl ether was required); the mixture was allowed to stand at room temperature overnight. Yield: 50 mg (79% based on Au) after recrystallization. It is soluble in alcohols, dichloromethane, chloroform, and acetone, is insoluble in saturated hydrocarbons and diethyl ether, and is air, light, and moisture stable both in the solid state and in solution. $[(PPh_3)Pt(AuPPh_3)_6](NO_3)_2$ has spectroscopic properties identical with those of $[(PPh_3)Pt(AuPPh_3)_6](BPh_4)_2$.[5] $^{31}P$ NMR ($CH_2Cl_2$, 25 °C): $\delta$ 50.3 (d with $^{195}Pt$ satellites, $^3J_{P-P} = 30$ Hz, $^2J_{^{195}Pt-P} = 413$ Hz, int = 6), 62.3 (m with $^{195}Pt$ satellites, $^3J_{P-P} = 30$ Hz, $J_{^{195}Pt-P} = 3766$ Hz, int = 1). Anal. Calcd for $Au_6PtP_7C_{126}H_{105}N_2O_6$: C, 45.35; H, 3.16; P, 6.50; N, 0.89. Found: C, 45.14; H, 3.16; P, 6.59; N, 0.76.

**Table I.** Crystallographic Data for $[(PPh_3)Pt(AuPPh_3)_6](NO_3)_2 \cdot Et_2O$ ($\mathbf{1}(NO_3)_2 \cdot Et_2O$) and $[(PPh_3)(CO)Pt(AuPPh_3)_6](PF_6)_2$ ($\mathbf{2}(PF_6)_2$)[a]

| Crystal Parameters and Measurement of Intensity Data | | |
|---|---|---|
| compd | $\mathbf{1}(NO_3)_2 \cdot Et_2O$ | $\mathbf{2}(PF_6)_2$[a] |
| space group | $P\bar{1}$ (No. 2) | $P\bar{1}$ (No. 2) |
| cell params at $T$, °C | −90 | −84 |
| $a$, Å | 14.158 (19) | 14.33 (1) |
| $b$, Å | 16.486 (22) | 16.80 (2) |
| $c$, Å | 27.091 (23) | 28.20 (3) |
| $\alpha$, deg | 94.92 (9) | 87.84 (9) |
| $\beta$, deg | 89.84 (9) | 82.47 (8) |
| $\gamma$, deg | 101.23 (11) | 66.96 (6) |
| $V$, Å$^3$ | 6179 (25) | 6197 (21) |
| $Z$ | 2 | 2 |
| calcd density, g cm$^{-3}$ | 1.833 | 1.891 |
| abs coeff, cm$^{-1}$ | 83.7 | 84.1 |
| max, min trans factors | 1.00, 0.68 | 1.69, 0.72 |
| formula | $C_{130}H_{115}N_2O_7P_7Au_6Pt$ | $C_{127}H_{105}F_{12}OP_9Au_6Pt$ |
| fw | 3410.67 | 3529.9 |
| radiation | Mo K$\alpha$ ($\lambda$ = 0.71069 Å) graphite monochromatized | |
| Refinement by Full-Matrix Least Squares | | |
| $R$[b] | 0.053 | 0.088 |
| $R_w$[b] | 0.067 | 0.099 |

[a] Solvent molecules were not located clearly in the X-ray analysis, so their number in the formula could not be determined (see Experimental Section). [b] The function minimized was $\sum w(|F_o| - |F_c|)^2$, where $w = 4F_o^2/\sigma_2(F_o)^2$. The unweighted and weighted residuals are defined as $R = \sum(||F_o| - |F_c||)/\sum|F_o|$ and $R_w = [(\sum w(|F_o| - |F_c|)^2)/(\sum w|F_o|^2)]^{1/2}$.

**$\mathbf{[(PPh_3)(CO)Pt(AuPPh_3)_6](PF_6)_2}$ ($\mathbf{2(PF_6)_2}$)** was prepared by dissolving complex $\mathbf{1}(NO_3)_2$ (100 mg, $3.00 \times 10^{-2}$ mmol) in 10 mL of dichloromethane and placing the solution under 1 atm of CO. The solution was stirred, and the color changed from dark brown to bright red immediately. The solution was reduced in volume to 2 mL under vacuum and transferred to a flask containing 60 mL of diethyl ether. A bright orange precipitate of $\mathbf{2}(NO_3)_2$ formed immediately. The precipitate was collected on a fritted filter, washed with 40 mL of diethyl ether, and dried under vacuum. Yield: 97 mg (96%). It is soluble in alcohols, dichloromethane, chloroform, and acetone, is insoluble in saturated hydrocarbons and diethyl ether, and is air, light, and moisture stable both in the solid state and in solution. The isotopically labeled analogue, $[(PPh_3)(^{13}CO)Pt(AuPPh_3)_6](NO_3)_2$, was prepared by the same procedure using $^{13}CO$. The $PF_6^-$ salt of **2** was made by metathesis of the $NO_3^-$ salt from a methanol solution containing $NH_4PF_6$. X-ray-quality crystals were obtained by slow solvent diffusion of $Et_2O$ into a $CH_2Cl_2$ solution containing **2**. $^{31}P$ NMR (acetone, 25 °C): $\delta$ 48.0 (d with $^{195}Pt$ satellites, $^3J_{P-P} = 28$ Hz, $^2J_{^{195}Pt-P} = 385$ Hz, int = 6), 47.3 (m with $^{195}Pt$ satellites, $^3J_{P-P} = 28$ Hz, $J_{1^{1}9_{5}Pt-P} = 2469$ Hz, int = 1). $^{13}C$ NMR (acetone-$d_6$, 25 °C): $\delta$ 208.2 (septet with $^{195}Pt$ satellites, $J_{^{195}Pt-^{13}C} = 1200$ Hz, $^2J_{^{13}C-P} = 4.2$ Hz, $^3J_{^{13}C-P} = 14.2$ Hz). IR (KBr): $\nu$(CO) 1967 cm$^{-1}$, $\nu(^{13}CO)$ 1922 cm$^{-1}$ [$\nu(CO)/\nu(^{13}CO) = 1.023$]. The equivalent conductance (192.9 cm$^2$ mhos mol$^{-1}$) is indicative of a 1:2 electrolyte in $CH_3CN$ solution. FABMS (*m*-nitrobenzyl alcohol matrix, $(Au_6Pt(PPh_3)_7(CO) = M^+)$: $m/z$ 3212 ($(M - CO)^+$), 3101 ($(M - PPh_3 + 2NO_3)^+$), 3012 ($(M - PPh_3 - CO + NO_3)^+$), 2978 ($(M - PPh_3)^+$), 2950 ($(M - PPh_3 - CO)^+$), 2753 ($(M - Au - PPh_3 - CO)^+$), 2688 ($(M - 2PPh_3 - CO)^+$). Anal. Calcd for $Au_6PtP_9C_{127}H_{105}F_{12}O$: C, 43.23; H, 3.00; P, 7.89. Found: C, 43.80; H, 2.92; P, 7.94.

**$\mathbf{[(PPh_3)(CO)Pt(AuPPh_3)_5]^+}$ (3)** was prepared either of two ways.

**Method a.** The $NO_3^-$ salt of **3** was prepared by dissolving complex $\mathbf{2}(NO_3)_2$ (160 mg, $4.76 \times 10^{-2}$ mmol) and $PPh_3$ (125 mg, $4.76 \times 10^{-1}$ mmol) in 20 mL of dichloromethane and stirring under 1 atm of CO at 25 °C for 2 h. The volume of the solution was reduced to 3 mL under vacuum, and 60 mL of diethyl ether was added to precipitate a dark red solid. The solid was collected on a fritted filter, washed with 50 mL of diethyl ether, and dried under vacuum. The in situ spectroscopic measurements indicated a complete reaction had taken place, with the additional formation of $Au(PPh_3)_2^+$. During purification, however, a small amount of **2** was re-formed by the apparent dissociation of $PPh_3$ from the $Au(PPh_3)_2^+$ byproduct followed by the addition of $AuPPh_3^+$. The $PF_6^-$ salt of **3** was made in an analogous manner.

**Method b.** The $Cl^-$ salt of **3** was prepared by stirring $[(PPh_3)Pt(AuPPh_3)_6]Cl_2$ ($\mathbf{1}Cl_2$) in $CH_2Cl_2$ under an atmosphere of CO. Complex $\mathbf{1}(NO_3)_2$ (150 mg, $4.50 \times 10^{-2}$ mmol) was dissolved in 4 mL of methanol. The solution was added dropwise to a stirred solution containing $NH_4Cl$ (602 mg, 11.25 mmol) in 3 mL of water and 20 mL of methanol. After the mixture was stirred for 20 min at 25 °C, 30 mL of water was added to precipitate $[(PPh_3)Pt(AuPPh_3)_6](Cl)_2$ as a yellow solid. This solid was isolated on a fritted-glass filter, washed with 10 mL of water followed by 20 mL of $Et_2O$, and dried under vacuum. $\mathbf{1}Cl_2$ was dissolved in 10 mL of $CH_2Cl_2$, and this solution was stirred under 1 atm of CO at 25 °C. After 30 min, the solvent was removed under vacuum, leaving a dark red solid, which was dissolved in 20 mL of benzene and left standing in a Schlenk tube. After 8 h, red needle-shaped crystals formed. The crystals were isolated on a fritted-glass filter, washed with 10 mL of benzene and 10 mL of hexanes, and dried under vacuum. Yield: 65 mg, 51.9%. It is soluble in alcohols, dichloromethane, chloroform, and acetone, is insoluble in saturated hydrocarbons and diethyl ether, and is air, light, and moisture stable both in the solid state and in solution. The isotopically labeled analogue, $[(PPh_3)(^{13}CO)Pt(AuPPh_3)_5]Cl$, was prepared by the same procedure using $^{13}CO$. The spectroscopic properties are identical for the three complexes of **3**. $^{31}P$ NMR ($CH_2Cl_2$, 25 °C): $\delta$ 47.9 (d, $^3J_{P-P} = 32$ Hz, $^2J_{^{195}Pt-P} = 448$ Hz, int = 5), 52.0 (sextet, $^3J_{P-P} = 32$ Hz, $J_{^{195}Pt-P} = 2808$ Hz, int = 1). $^{13}C$ NMR ($CDCl_3$, 25 °C): 208.4

---

(26) Fumagalli, A.; Martinengo, S.; Albano, V. G.; Braga, D. *J. Chem. Soc., Dalton Trans.* **1988**, 1237.
(27) Carriedo, G. A.; Riera, V.; J. Sânchez, G.; Solans, X. *J. Chem. Soc., Dalton Trans.* **1988**, 1957.
(28) Housecraft, C. E.; Shongwe, M. S.; Rheingold, A. L. *Organometallics* **1988**, *7*, 1885.
(29) Teo, B. K.; Hong, M.; Zhang, H.; Huang, D.; Shi, X. *J. Chem. Soc., Chem. Commun.* **1988**, 204.
(30) Drake, S. R.; Johnson, B. F. G.; Lewis, J. *J. Organomet. Chem.* **1988**, *340*, C31.
(31) Green, M.; Howard, J. A. K.; James, A. P.; Nunn, C. M.; Stone, F. G. A. *J. Chem. Soc., Dalton Trans.* **1987**, 61.
(32) Low, A. A.; Lauher, J. W. *Inorg. Chem.* **1987**, *26*, 3863.
(33) Bruce, M. I.; Williams, M. L.; Patrick, J. M.; Skelton, B. W.; White, A. H. *J. Chem. Soc., Dalton Trans.* **1986**, 2557.
(34) Deeming, A. J.; Donovan-Mtunzi, S.; Hardcastle, K. *J. Chem. Soc., Dalton Trans.* **1986**, 543.
(35) Puga, J.; Sânchez-Delgado, R. A.; Ascanio, J.; Braga, D. *J. Chem. Soc., Chem. Commun.* **1986**, 1631.
(36) Farrugia, L. J. *Acta Crystallogr.* **1986**, *C42*, 680.
(37) Arsenault, G. J.; Anderson, C. M.; Puddephatt, R. J. *Organometallics* **1988**, *7*, 2094.
(38) Sinfelt, J. H. *Bimetallic Catalysts*; Wiley: New York, 1983; Chapters 1 and 2.
(39) Evans, J.; Jingxing, G. *J. Chem. Soc., Chem. Commun.* **1985**, 39.
(40) Schwank, J. *Gold Bull.* **1985**, *18*, 2; **1983**, *16*, 103.
(41) Wachs, I. E. *Gold Bull.* **1983**, *16*, 98.
(42) Sermon, P. A.; Thomas, J. M.; Keryou, K.; Millward, G. R. *Angew. Chem., Int. Ed. Engl.* **1987**, *26*, 918.
(43) Exxon Research and Engineering Co. Eur. Pat. 37700, 1981; U.S. Pat. 4,301,086, 1981; U.S. Pat. 4,342,838, 1982.
(44) Union Carbide Corp. U.S. Pat. 3,878,292, 1975.
(45) Braunstein, P.; Rosé, J. In *Stereochemistry of Organometallic and Inorganic Compounds*; Bernal, I., Ed.; Elsevier: Amsterdam, 1989; Vol. 3 and references cited therein.
(46) Green, M.; Howard, J. A. K.; Spencer, J. L.; Stone, F. G. A. *J. Chem. Soc., Dalton Trans.* **1977**, 271.

(sextet with $^{195}$Pt satellites, $J_{^{195}\mathrm{Pt}-^{13}\mathrm{C}}$ = 1330 Hz, $^2J_{^{13}\mathrm{C-P}}$ = 3.0 Hz, $^3J_{^{13}\mathrm{C-P}}$ = 13.2 Hz). IR (KBr): ν(CO) 1946 cm$^{-1}$, ν($^{13}$CO) 1900 cm$^{-1}$ [ν(CO)/ν($^{13}$CO) = 1.024]. The equivalent conductance of the Cl$^-$ salt (81.5 cm$^2$ mhos mol$^{-1}$) is indicative of a 1:1 electrolyte in $CH_3CN$ solution. FABMS (*m*-nitrobenzyl alcohol matrix) of the Cl$^-$ salt: *m*/*z* 2781 ($Au_5Pt(PPh_3)_6(CO)$ = M$^+$), 2753 ((M − CO)$^+$), 2519 ((M − $PPh_3$)$^+$), 2491 ((M − $PPh_3$ − CO)$^+$), 2294 ((M − Au − $PPh_3$ − CO)$^+$), 2032 ((M − Au − 2$PPh_3$ − CO)$^+$).

**X-ray Structure Determinations. Collection and Reduction of X-ray Data.** A summary of crystal data is presented in Table I. A rectangular crystal of $[(PPh_3)Pt(AuPPh_3)_6](NO_3)_2{\cdot}Et_2O$ (**1**$(NO_3)_2{\cdot}Et_2O$) was coated with a viscous high molecular weight hydrocarbon and secured on a glass fiber by cooling to −90 °C. The crystal class and space group were unambiguously determined by the Enraf-Nonius CAD4-SDP-PLUS peak search, centering, and indexing programs[47] and by the successful solution and refinement of the structure (vide infra). The intensities of three standard reflections were measured every 1.5 h of X-ray exposure time during data collection. Compound **1** decayed as a linear function of X-ray exposure time with a total decrease of 3.4%. A linear correction was applied with the SDP program DECAY by using maximum and minimum correction factors of 1.018 and 1.000.[47] The data were corrected for Lorentz, polarization, and background effects. An empirical adsorption correction was applied by use of ψ-scan data and the program EAC.[47]

A red, rectangular crystal of $[(PPh_3)(CO)Pt(AuPPh_3)_6](PF_6)_2$ (**2**$(PF_6)_2$) was similarly coated with a viscous high molecular weight hydrocarbon and secured on a glass fiber by cooling to −84 °C. The outer layers of the crystal decomposed somewhat, but this stabilized after several hours. Data collection was carried out with this crystal anyway because of repeated previous failures to find a suitable crystal. Solvent loss from these crystals was so rapid that we were very lucky to collect a data set. All data were collected by using an Enraf-Nonius CAD4 diffractometer with controlling hardware and software,[48] and all calculations were performed by using the Molecular Structure Corp. TEXSAN crystallographic software package,[49] run on a Microvax 3 computer. The crystal class and space group were determined on the basis of the lack of systematic absences, packing considerations, a statistical analysis of intensity distribution, and the successful solution and refinement of the structure (vide infra). The intensities of three standard reflections were measured every 1.5 h of X-ray exposure time during data collection. No decay was observed once data collection was begun. The data were corrected for Lorentz, polarization, and background effects. An empirical absorption correction was applied by use of the program DIFABS.[50]

**Solution and Refinement of the Structures.** The structure of **1**$(NO_3)_2$ was solved by conventional heavy-atom techniques. The metal atoms were located by Patterson syntheses. The structure of **2**$(PF_6)_2$ was solved by direct methods.[51,52] Full-matrix least-squares refinement and difference Fourier calculations were used to locate all remaining non-hydrogen atoms. The atomic scattering factors were taken from the usual tabulation,[53] and the effects of anomalous dispersion were included in $F_c$ by using Cromer and Iber's values of $\Delta f'$ and $\Delta f''$.[54] All of the nonmetal atoms were refined with isotropic thermal parameters for both structures. The phenyl carbon atoms and the $PF_6^-$ fluorine atoms in **2** were refined in rigid groups with continuous isotropic temperature factors for each group. One $Et_2O$ solvent molecule for **1** was located and refined. There were a few other small peaks observed in the final difference Fourier map of **1**, but they did not refine well and were not included. These peaks were well separated from refined atom positions and are probably disordered solvent. In **2** there was significant electron density in a region well removed from the cluster dication and $PF_6^-$ anions. This was due to disordered and partially occupied solvent molecules ($CH_2Cl_2$ and $Et_2O$). These peaks did not refine well, and reasonable models for the solvent molecules could not be found. These peaks were therefore omitted from the refinement. Such disordered behavior of solvent molecules in large cluster compounds is common and generally has little

**Table II.** Positional Parameters and Their Estimated Standard Deviations for Core Atoms in $[(PPh_3)Pt(AuPPh_3)_6](NO_3)_2{\cdot}Et_2O$ (**1**$(NO_3)_2{\cdot}Et_2O$)[a]

| atom | *x* | *y* | *z* | *B*, Å$^2$ |
|---|---|---|---|---|
| Pt | 0.01145 (6) | 0.21166 (5) | 0.23770 (3) | 1.06 (2) |
| Au1 | −0.11069 (6) | 0.20511 (5) | 0.31410 (3) | 1.32 (2) |
| Au2 | −0.03329 (7) | 0.35759 (5) | 0.26884 (3) | 1.40 (2) |
| Au3 | −0.16675 (6) | 0.23480 (5) | 0.21558 (4) | 1.45 (2) |
| Au4 | −0.00496 (6) | 0.30612 (5) | 0.16423 (3) | 1.32 (2) |
| Au5 | −0.00933 (7) | 0.07139 (5) | 0.28223 (3) | 1.52 (2) |
| Au6 | 0.08929 (6) | 0.21669 (5) | 0.32804 (3) | 1.38 (2) |
| P1 | −0.2178 (4) | 0.1840 (4) | 0.3786 (2) | 1.7 (1)* |
| P2 | −0.0076 (4) | 0.4973 (4) | 0.2923 (2) | 1.6 (1)* |
| P3 | −0.3220 (4) | 0.1897 (4) | 0.1883 (2) | 1.7 (1)* |
| P4 | −0.0114 (4) | 0.3822 (4) | 0.0973 (2) | 1.6 (1)* |
| P5 | −0.0316 (5) | −0.0680 (4) | 0.2913 (3) | 2.0 (1)* |
| P6 | 0.1941 (4) | 0.2684 (4) | 0.3924 (2) | 1.5 (1)* |
| P | 0.1142 (4) | 0.1676 (4) | 0.1813 (2) | 1.5 (1)* |

[a] Counterion, solvent molecule, and phenyl group positional parameters are provided in the supplementary material. Starred values indicate atoms were refined isotropically. Anisotropically refined atoms are given in the form of the isotropic equivalent thermal parameter defined as $(4/3)[a^2\beta(1,1) + b^2\beta(2,2) + c^2\beta(3,3) + ab(\cos\gamma)\beta(1,2) + ac(\cos\beta)\beta(1,3) + bc(\cos\alpha)\beta(2,3)]$.

**Table III.** Positional Parameters and Their Estimated Standard Deviations for Core Atoms in $[(PPh_3)(CO)Pt(AuPPh_3)_6](PF_6)_2$ (**2**$(PF_6)_2$)[a]

| atom | *x* | *y* | *z* | *B*, Å$^2$ |
|---|---|---|---|---|
| Pt | 0.4275 (1) | 0.02012 (8) | 0.70960 (6) | 1.0 (1) |
| Au1 | 0.3242 (1) | −0.07114 (8) | 0.75046 (6) | 1.2 (1) |
| Au2 | 0.3082 (1) | 0.09595 (9) | 0.79016 (6) | 1.4 (1) |
| Au3 | 0.2286 (1) | 0.09089 (9) | 0.70016 (6) | 1.3 (1) |
| Au4 | 0.3465 (1) | 0.19418 (9) | 0.71290 (6) | 1.6 (1) |
| Au5 | 0.5339 (1) | −0.15375 (8) | 0.70679 (6) | 1.3 (1) |
| Au6 | 0.4913 (1) | −0.05518 (9) | 0.79230 (6) | 1.4 (1) |
| P1 | 0.2302 (8) | −0.1486 (6) | 0.7796 (4) | 1.8 (2) |
| P2 | 0.2209 (8) | 0.1723 (6) | 0.8583 (4) | 1.5 (2) |
| P3 | 0.0746 (8) | 0.1387 (6) | 0.6705 (4) | 1.7 (2) |
| P4 | 0.3443 (9) | 0.3320 (7) | 0.7089 (4) | 2.2 (2) |
| P5 | 0.6477 (7) | −0.2926 (6) | 0.6884 (4) | 1.1 (2) |
| P6 | 0.5984 (8) | −0.0969 (6) | 0.8504 (4) | 1.5 (2) |
| P | 0.4573 (7) | 0.0006 (6) | 0.6263 (4) | 1.1 (2) |
| C | 0.540 (4) | 0.055 (3) | 0.720 (2) | 4 (1) |
| O | 0.603 (3) | 0.072 (2) | 0.722 (1) | 4.1 (7) |

[a] See footnote in Table II.

**Scheme I**

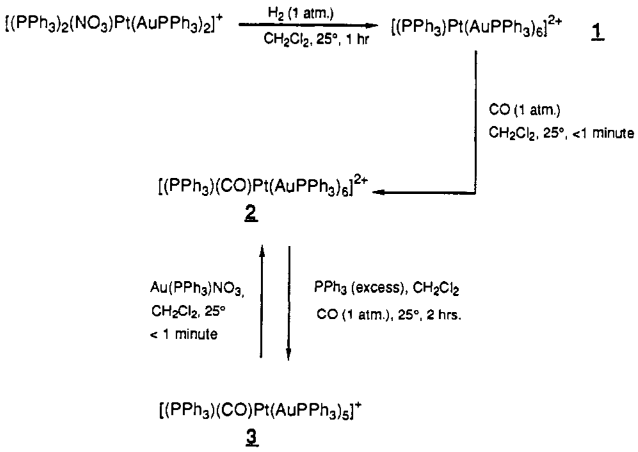

---

[47] All calculations on the analysis of **1** were carried out on PDP 8A and 11/34 computers with use of the Enraf-Nonius CAD4-SDP programs. This crystallographic computing package is described by: Frenz, B. A. In *Computing in Crystallography*; Schenk, H., Olthoff-Hazelkamp, R., von Koningsveld, H., Bassi, G. C., Eds.; Delft University Press: Delft, Holland, 1978; pp 64–71. *CAD 4 User's Manual*; Enraf-Nonius: Delft, Holland, 1978.

[48] Schagen, J. D.; Straver, L.; van Meurs, F.; Williams, G. Enraf-Nonius Delft, Scientific Instruments Division: Delft, The Netherlands, 1988.

[49] All calculations on the analysis of **2** were carried out with use of the Molecular Structure Corp. TEXSAN-TEXRAY Structure Analysis Package, version 2.1, 1985.

[50] Walker, N.; Stuart, D. *Acta Crystallogr.* **1983**, *A39*, 158.

[51] MITHRIL (an integrated direct methods computer program); University of Glasgow, Scotland. Gilmore, C. J. *J. Appl. Crystallogr.* **1984**, *17*, 42.

[52] DIRDIF (Direct Methods for Difference Structures; an automatic procedure for phase extension and refinement of difference structure factors): Beurskens, P. T. Technical Report 1984/1, Crystallography Laboratory: Toernooiveld, 6525 Ed Nijmegen, The Netherlands, 1984.

[53] Cromer, D. T.; Waber, J. T. In *International Tables for X-ray Crystallography*; Kynoch: Birmingham, England, 1974; Vol. IV, Table 2.2.4.

[54] Cromer, D. T. In *International Tables for X-ray Crystallography*; Kynoch: Birmingham, England, 1974; Vol. IV, Table 2.3.1.

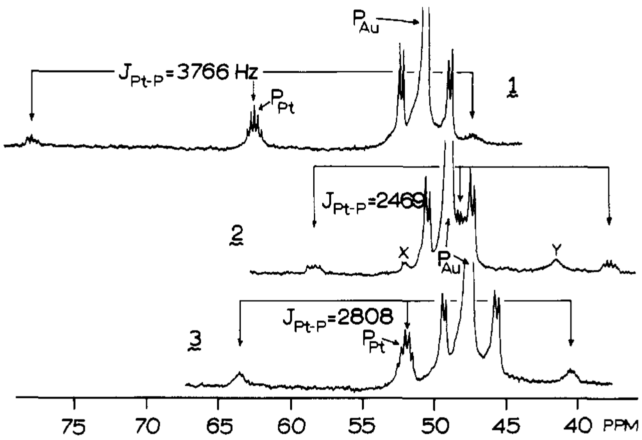

**Figure 1.** $^{31}$P NMR spectra of $[(PPh_3)Pt(AuPPh_3)_6]^{2+}$ (**1**) (upper trace), $[(PPh_3)(CO)Pt(AuPPh_3)_6]^{2+}$ (**2**) (middle trace), and $[(PPh_3)(CO)Pt(AuPPh_3)_5]^{+}$ (**3**) (lower trace) in solution recorded at 25 °C with the use of $CH_2Cl_2$, acetone, and $CH_2Cl_2$, respectively, as solvent (internal standard trimethyl phosphate, $\delta = 0$). The central doublet due to the $Au(PPh_3)$ phosphorus has been cut off for clarity. The peaks labeled X and Y are due to $[(PPh_3)Pt(AuPPh_3)_6]^{2+}$ and $Au(PPh_3)_2^{+}$, respectively.

effect on the structure of the cluster. The anions were located and refined for both structures, but one of the $PF_6^-$ anions in **2** showed signs of disorder. The positions of the hydrogen atoms in the $PPh_3$ ligands were not included in the structure factor calculations of either structure. The largest peak in the final difference Fourier map of **1** was ca. 3.3 e Å$^{-3}$ and was located near one of the nitrate counterions. The largest peaks for **2** were of similar magnitude and were located in the region of disordered solvent. The final positional and thermal parameters in the refined atoms within the coordination core for **1** and **2** are given in Tables II and III, respectively. ORTEP drawings of **1** and **2** including the labeling scheme and selected distances and angles are shown in Figures 2 and 3. A complete listing of thermal parameters, positional parameters, distances, angles, least-squares planes, and structure factor amplitudes are included as supplementary material.[55]

## Results

The transformations observed in this study are summarized in Scheme I. $^{31}$P and $^{13}$C NMR spectra are shown in Figures 1 and 6, respectively. These spectra and other characterizing data are considered in the Discussion.

## Discussion

**$[(PPh_3)Pt(AuPPh_3)_6]^{2+}$ (1).** We have previously reported[5] that $CH_2Cl_2$ solutions of $[(PPh_3)_2(NO_3)Pt(AuPPh_3)_2]NO_3$ reacted with $H_2$ to form a brown microcrystalline solid, which was characterized as $[(PPh_3)Pt(AuPPh_3)_6](NO_3)_2$. The $^{31}$P NMR spectrum ($CH_2Cl_2$) as shown in the upper trace of Figure 1 consists of a large doublet at $\delta$ 50.3 ($^3J_{P-P}$ = 30 Hz) with $^{195}$Pt satellites ($^2J_{^{195}Pt-P}$ = 413 Hz) and a small multiplet at $\delta$ 62.3 interpreted as a septet ($^3J_{P-P}$= 30 Hz) with $^{195}$Pt satellites ($^2J_{^{195}Pt-P}$ = 3766 Hz). Integration of the small multiplet vs the central doublet gave a ratio of 1:6 ± 0.5). $^1$H NMR spectroscopy showed no evidence for hydride ligands. Positive-ion FABMS analysis of the $BPh_4^-$ salt of this complex gave a spectrum with well-resolved peaks. An analysis of the isotopic ion distribution pattern for the highest mass peak gave a most abundant mass ion of 3531.7, which corresponded to the ion $[Au_6Pt(PPh_3)_7(BPh_4)]^+$.[5] A complete analysis of the fragmentation pattern suggested that the neutral compound was $[(PPh_3)Pt(AuPPh_3)_6](BPh_4)_2$.

X-ray-quality crystals of the $NO_3^-$ salt of $[(PPh_3)Pt(AuPPh_3)_6]^{2+}$ have since been obtained, and a single-crystal X-ray diffraction analysis was carried out in order to determine the nature of the gold–platinum interactions and the overall structure of the complex. These questions could not be answered from the FABMS, solution NMR, and IR data alone.

The structure of the coordination core of **1** with selected distances and angles is shown in Figure 2. The structure consists of six $Au(PPh_3)$ units bonded to a $Pt(PPh_3)$ unit. The Pt atom and four of the Au atoms (Au1, Au2, Au3 and Au4) form a trigonal bipyramid (TBP) with Pt, Au2, and Au3 forming the equatorial trigonal plane with Au1 and Au4 in the axial positions. This TBP grouping shares an edge (Pt–Au1) with a tetrahedral grouping formed by the Pt atom and three of the Au atoms (Au1, Au5, and Au6). One $PPh_3$ ligand is bonded to the centrally located Pt atom. A further discussion of the structure of **1** is presented below.

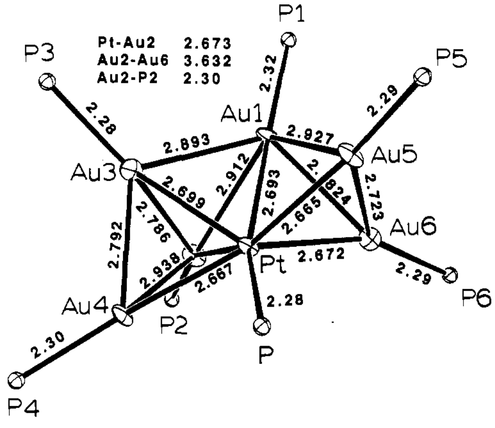

**Figure 2.** ORTEP drawing of the coordination core of **1** with selected bond distances (Å). Ellipsoids are drawn with 50% probability boundaries. Phenyl rings have been omitted for clarity. Selected angles (deg) are as follows, wherein numbers refer to respective Au atoms: Pt–1–P1, 173.8 (1); Pt–2–P2, 157.4 (1); Pt–3–P3, 153.1 (1); Pt–4–P4, 175.6 (1); Pt–5–P5, 159.3 (2); Pt–6–P6, 155.9 (1); 1–Pt–2, 65.73 (3); 1–Pt–3, 64.89 (3); 1–P–4, 120.65 (3); 1–Pt–5, 66.23 (3); 1–Pt–6, 63.51 (3); 2–Pt–3, 62.46 (3); 2–Pt–4, 66.75 (3); 2–Pt–5, 130.09 (4); 2–Pt–6, 85.59 (3); 3–Pt–4, 62.71 (3); 3–Pt–5, 107.26 (3); 3–Pt–6, 126.92 (4); 4–Pt–5, 156.24 (4); 4–Pt–6, 142.33 (4); 5–Pt–6, 61.35 (3); 1–Pt–P7, 158.1 (1); 2–Pt–P7, 135.7 (1); 3–Pt–P7, 124.5 (1); 4–Pt–P7, 78.8 (1); 5–Pt–P7, 91.9 (1); 6–Pt–P7, 108.2 (1). Average esd's for Au–Pt, Au–Au, Au–P, and Pt–P distances are 0.001, 0.001, 0.01, and 0.01 Å, respectively.

The addition of LiC≡CPh to a THF slurry containing **1** yielded a product characterized as $[(PPh_3)(C{\equiv}CPh)Pt(AuPPh_3)_6]^+$ [$^{31}$P NMR ($CH_2Cl_2$, 25 °C): $\delta$ 59.4 (Pt*P*, m, $^3J_{P-P}$ = 40 Hz, $J_{^{195}Pt-P}$ unobserved), 43.0 (Au*P*, d, $^3J_{P-P}$ = 40 Hz, $^2J_{^{195}Pt-P}$ = 437 Hz). IR (KBr): $\nu$(CC) 2044 cm$^{-1}$]. The spectroscopic characteristics of this complex are very similar to those of $[(PPh_3)(C{\equiv}C\text{-}t\text{-}Bu)(AuPPh_3)_6]^+$ [$^{31}$P NMR (acetone, 25 °C): $\delta$ 59.0 (septet, $^3J_{P-P}$ = 41 Hz, $J_{^{195}Pt-P}$ = 2154 Hz), 42.5 (d, $^3J_{P-P}$ = 41 Hz, $^2J_{^{195}Pt-P}$ = 444 Hz)].[18]

**$[(PPh_3)(CO)Pt(AuPPh_3)_6]^{2+}$ (2)** was prepared by the exposure of a solution of **1** to 1 atm of CO with use of $CH_2Cl_2$ as solvent. The characterization data are consistent with the formulation of **2** as the carbonyl adduct of **1** with one $PPh_3$ and one CO ligand bonded to the Pt atom. This reaction is analogous to the reaction of $[Pt(AuPPh_3)_8](NO_3)_2$ with CO, which yielded $[(CO)Pt(AuPPh_3)_8](NO_3)_2$.[7] These $Au_8Pt$ complexes, however, do not have a $PPh_3$ ligand bonded to the central Pt atom. The $^{31}$P NMR spectrum (25 °C, acetone-$d_6$) of **2**, which is displayed in the middle trace of Figure 1, showed two groups of resonances centered at $\delta$ 48.0 and 47.3 with a relative intensity of 6:1. The peak assigned to the Pt phosphines appeared at $\delta$ 47.3 as a multiplet ($^3J_{P-P}$ = 28 Hz) with $^{195}$Pt satellites ($J_{^{195}Pt-P}$ = 2469 Hz). The downfield resonance at $\delta$ 48.0 is assigned to the Au phosphines and appears as a doublet ($^3J_{P-P}$ = 28 Hz) with $^{195}$Pt satellites ($^2J_{^{195}Pt-P}$ = 385 Hz). This indicates that the $Au(PPh_3)$ units are equivalent on the NMR time scale; however, the low-temperature (−90 °C) solution NMR spectrum did not further resolve the spectrum. Fluxional behavior was also observed for complex **1** and $[(PPh_3)(C{\equiv}C\text{-}t\text{-}Bu)Pt(AuPPh_3)_6]^+$.[18]

The $^{13}$C NMR solution spectrum (acetone-$d_6$, 25 °C) of isotopically labeled $[(PPh_3)(^{13}CO)Pt(AuPPh_3)_6](NO_3)_2$ consisted of a septet at $\delta$ 208.2 ($^2J_{^{13}C-P}$ = 4.2 Hz, $^3J_{^{13}C-P}$ = 14.2 Hz) with $^{195}$Pt satellites ($J_{^{195}Pt-^{13}C}$ = 1200 Hz). The chemical shift and coupling constants are similar to those of $[(CO)Pt(AuPPh_3)_8](NO_3)_2$ ($\delta$ 210.7, $J_{^{195}Pt-^{13}C}$ = 1256 Hz, $^3J_{^{13}C-P}$ = 11 Hz).[7] The IR

---

(55) See paragraph at end of paper regarding supplementary material.

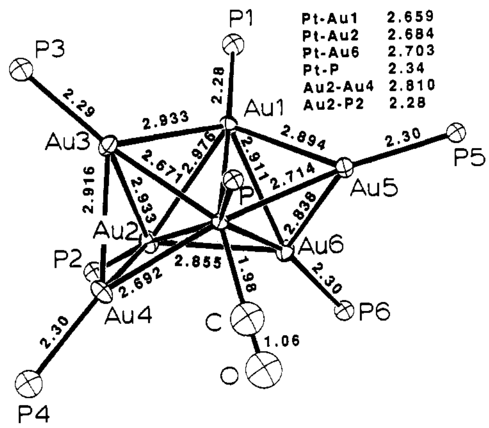

Figure 3. ORTEP drawing of the coordination core of **2** with selected bond distances (Å). Ellipsoids are drawn with 50% probability boundaries. Phenyl rings have been omitted for clarity. Selected angles (deg) are as follows, wherein numbers refer to respective Au atoms: Pt-1-P1, 175.2 (3); Pt-2-P2, 171.6 (3); Pt-3-P3, 164.0 (3); Pt-4-P4, 157.4 (3); Pt-5-P5, 165.6 (3); Pt-6-P6, 155.3 (3); 1-Pt-2, 67.70 (6); 1-Pt-3, 66.76 (6); 1-Pt-4, 121.39 (7); 1-Pt-5, 65.15 (5); 1-Pt-6, 65.74 (6); 2-Pt-3, 66.43 (6); 2-Pt-4, 63.03 (5); 2-Pt-5, 119.40 (7); 2-Pt-6, 64.01 (5); 3-Pt-4, 65.86 (6); 3-Pt-5, 121.88 (8); 3-Pt-6, 120.65 (8); 4-Pt-5, 172.23 (9); 4-Pt-6, 114.47 (8); 5-Pt-6, 63.19 (6); 1-Pt-P, 111.3 (3); 2-Pt-P, 151.7 (2); 3-Pt-P, 86.9 (2); 4-Pt-P, 98.5 (2); 5-Pt-P, 81.9 (2); 6-Pt-P, 143.1 (2); Pt-C-O, 175 (4); 1-Pt-C, 141 (1); 2-Pt-C, 95 (1); 3-Pt-C, 140 (1); 4-Pt-C, 74 (1); 5-Pt-C, 98 (1); 6-Pt-C, 75 (1); P-Pt-C, 100 (2). Average esd's for Au-Pt, Au-Au, Au-P, Pt-P, Pt-C, and C-O distances are 0.002, 0.002, 0.01, 0.01, 0.06, and 0.07 Å, respectively.

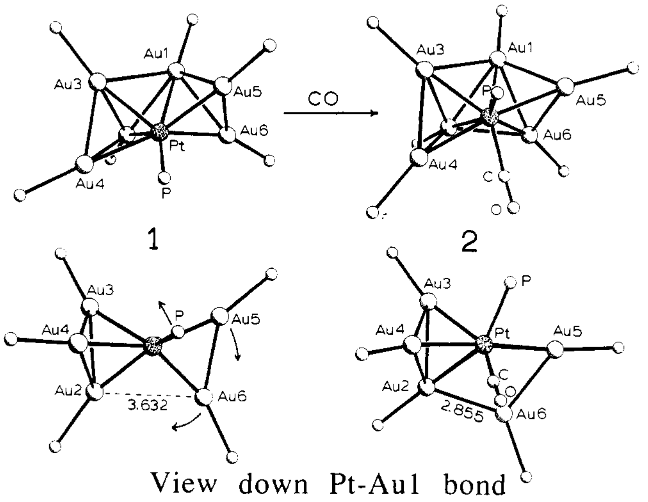

Figure 4. PLUTO drawings of two perspectives of the cluster core of $[(PPh_3)Pt(AuPPh_3)_6]^{2+}$ and $[(PPh_3)(CO)Pt(AuPPh_3)_6]^{2+}$ showing the structural changes upon the addition of CO. The lower view is along the Pt-Au1 bond, and the arrows show the major shifts in atomic positions upon the addition of CO.

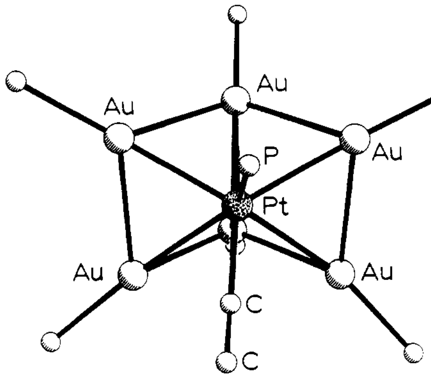

Figure 5. PLUTO drawing of the cluster core of $[(PPh_3(C{\equiv}C\text{-}t\text{-}Bu)Pt(AuPPh_3)_6]^+$ showing the large structural differences compared with $[(PPh_3)(CO)Pt(AuPPh_3)_6]^{2+}$. This latter compound is shown from a similar perspective in Figure 5 (upper right corner). See ref 18 for a discussion of the structure of $[(PPh_3)C{\equiv}C\text{-}t\text{-}Bu)Pt(AuPPh_3)_6]^+$. The *t*-Bu group is omitted for clarity.

spectrum (KBr) of **2** displayed a $\nu$(CO) absorption at 1967 cm$^{-1}$, which is consistent with a terminally bound metal carbonyl. The $\nu$(CO) absorption shifted to lower energy (1922 cm$^{-1}$) in the IR spectrum when **2** was synthesized with 99% $^{13}$CO.

Positive-ion FABMS analysis yielded a spectrum with well-resolved peaks. The peak corresponding to $M^+$ ($(Au_6Pt(PPh_3)_7(CO)^+$) at 3239 was very small and difficult to distinguish from the base-line noise; however, other peaks were present that represented fragments containing CO (see Experimental Section). An analysis of the fragmentation pattern of the spectrum supports the formulation of **2** as $[(PPh_3)(CO)Pt(AuPPh_3)_6]^{2+}$. In agreement with this formulation, the conductance of **2** in $CH_3CN$ showed it to be a 1:2 electrolyte.

Further support of the formulation of **2** as $[(PPh_3)(CO)Pt(AuPPh_3)_6]^{2+}$ comes from a study of its reactivity. Complex **2** reacted with $Pt(cod)_2$ with $CH_2Cl_2$ as solvent to remove the CO ligand and re-form **1**. This was evidenced by $^{31}$P and $^1$H NMR and IR spectroscopies.

X-ray-quality crystals of the $PF_6^-$ salt of $[(PPh_3)(CO)Pt(AuPPh_3)_6]^{2+}$ have been obtained, and a single-crystal X-ray diffraction analysis was carried out. The structure of the coordination core of **2** with selected distances and angles is shown in Figure 3. The $PtAu_6$ core structure is grossly similar to that of **1**. The central Pt atom has six $Au(PPh_3)$ units, a $PPh_3$ ligand, and a CO ligand bonded to it. The major structural changes upon the addition of CO to **1** in the formation of **2** are the change in the position of the $PPh_3$ ligand and the formation of one additional Au-Au bonding interaction. As shown in Figure 4, upon incorporation of the CO ligand, the $PPh_3$ ligand rotates up toward the Au1 atom and the Au5 and Au6 atoms rotate toward the Au2 atom. This results in the Au2-Au6 distance decreasing from 3.632 Å in **1** to a bonding distance of 2.855 Å in **2**. The two views in Figure 4 show this geometry change quite clearly.

**Structural Features of 1 and 2.** It is interesting to compare the structures of $[(PPh_3)Pt(AuPPh_3)_6]^{2+}$ (**1**) and $[(PPh_3)(CO)Pt(AuPPh_3)_6]^{2+}$ (**2**) to each other and to that of the acetylide adduct $[(PPh_3)(C{\equiv}C\text{-}t\text{-}Bu)Pt(AuPPh_3)_6]^+$ characterized by Puddephatt,[18] in which one $PPh_3$ ligand and the acetylide ligand are bonded to the Pt atom. This latter complex consists of a central platinum atom at the apex of two face-shared $Au_4Pt$ square pyramids (see Figure 5). **1** has a toroidal structure as predicted by its 88 total valence electrons.[56] The torus plane is perpendicular to the plane of the drawing in the lower view of Figure 4 (defined roughly through Au4, Au1, Pt, and P). Addition of CO or $C{\equiv}C\text{-}t\text{-}Bu^-$ increases the valence electron count to 90 electrons, implying a spheroidal structure, which can be seen for **2** in Figure 4 and for $[(PPh_3)(C{\equiv}C\text{-}t\text{-}Bu)Pt(AuPPh_3)_6]^+$ in Figure 5. The nearly cubic arrangement shown in Figure 5 is deformed in **2**, giving shorter contacts between Au2 and Au3 and between Au1 and Au6. The reason for this difference is not known but is most likely caused by electronic differences between the acetylide ligand and the carbon monoxide ligand. Neither the acetylide nor the CO ligand is considered to be sterically demanding in these compounds. To our knowledge, theories have not been put forth that account for the geometries of these complexes. A better understanding must wait for more structural information on related clusters.

The Au-Pt distances in **1** (average 2.678 Å, range 2.665-2.699 Å) and in **2** (average 2.687 Å, range 2.659-2.714 Å) are within the range of values, 2.600-3.028 Å,[1] observed in other Au-Pt clusters containing primarily phosphine ligands (for example, average 2.702 Å in $[(PPh_3)(H)Pt(AuPPh_3)_7](PF_6)_2$,[6] 2.635 Å in $[Pt(AuPPh_3)_8](NO_3)_2$,[8] 2.675 Å in $[(CO)Pt(AuPPh_3)_8](NO_3)_2$,[7] and 2.665 Å in the acetylide adduct $[(PPh_3)(C{\equiv}C\text{-}t\text{-}Bu)Pt(AuPPh_3)_6]^+$).[18] The Au-Au bond distances in **1** (average 2.849 Å, range 2.723-2.938 Å) and in **2** (average 2.896 Å, range

---

(56) Hall, K. P.; Gilmour, D. I.; Mingos, D. M. P. *J. Organomet. Chem.* **1984**, *268*, 275.

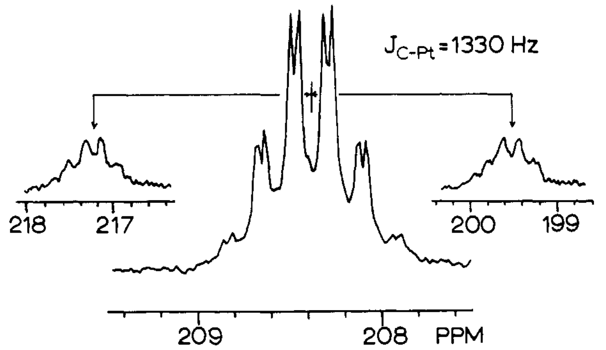

**Figure 6.** $^{13}$C NMR spectrum of $[(PPh_3)(CO)Pt(AuPPh_3)_5]^+$ (**3**) in solution recorded at 25 °C with the use of $CDCl_3$ as solvent. The $^{195}$Pt satellite peaks are shown on the same vertical scale, but the horizontal scale has been compressed for clarity.

2.810–2.976 Å) are within the range of values, 2.593–3.222 Å,[1] observed in other Au–Pt clusters containing primarily phosphine ligands (for example, average 2.938 Å in $[(PPh_3)(H)Pt(AuPPh_3)_7](PF_6)_2$,[6] 2.827 Å in $[Pt(AuPPh_3)_8](NO_3)_2$,[8] and 2.987 Å in $[(CO)Pt(AuPPh_3)_8](NO_3)_2)$,[7] and compare well to the Au–Au bond lengths in the acetylide adduct $[(PPh_3)(C{\equiv}C\text{-}t\text{-}Bu)Pt(AuPPh_3)_6]^+$ (average 2.854 Å, range 2.832–2.879 Å).[18]

The Pt–P distances in **1** (2.28 (1) Å) and in **2** (2.34 (1) Å) compare well to those in other Au–Pt clusters[6,18] and are within the range of values observed in platinum–phosphine complexes.[57] The Au–P distances in **1** (average 2.30 Å, range 2.28–2.32 Å) and in **2** (average 2.29 Å, range 2.28–2.30 Å) also generally compare well to those in other Au–Pt complexes.[6,7,18]

Two of the Au–$PPh_3$ vectors in **1** are approximately trans to the Pt atom (Pt–Au1–P1 173.8 (1)°, Pt–Au4–P4 175.6 (1)°), which is a general trend seen in complexes of this type;[1] however, the remaining Pt–Au–P vectors average 156.4° (range 153.1–159.3°). The overall Pt–Au–P angle in **1** is 162.5°. A similar deviation from linear Pt–Au–P bonding is noted in **2** (average angle 164.9°, range 155.3–175.2°). The Au–$PPh_3$ vectors in $[Au_6Pt(PPh_3)_7(CC\text{-}t\text{-}Bu)]^+$ are more transoid to the Pt atom (average 172.1°, range 163.8–177.9°).[18]

**$[Au_5Pt(PPh_3)_6(CO)]^+$ (3)** was synthesized by stirring a $CH_2Cl_2$ solution of $[(PPh_3)Pt(AuPPh_3)_6]Cl_2$ (**1**$Cl_2$) under 1 atm of CO. The other product of this reaction was $Au(PPh_3)Cl$. It is interesting to note that excess of $Cl^-$ did not remove any $Au(PPh_3)$ groups when added to a $CH_2Cl_2$ solution of **1** at room temperature over a period of days. Complex **3** was also synthesized with the $NO_3^-$ or $PF_6^-$ counterion by stirring solutions containing **1** with $PPh_3$ under 1 atm of CO; however, purification of the reaction mixture was difficult. The $^{31}$P NMR spectrum (25 °C, $CH_2Cl_2$) of **3**, as displayed in the lower trace of Figure 1, showed two resonances at $\delta$ 52.0 and 48.0 with a relative intensity of 1:5. The peak assigned to the $PPh_3$ ligand bound to the Pt atom ($\delta$ 52.0) appeared as a sextet ($^3J_{P-P}$ = 32 Hz) with $^{195}$Pt satellites ($J_{^{195}Pt-P}$ = 2808 Hz). The upfield resonance ($\delta$ 47.9) assigned to the $Au(PPh_3)$ ligands appeared as a doublet ($^3J_{P-P}$ = 32 Hz) with $^{195}$Pt satellites ($^2J_{^{195}Pt-P}$ = 448 Hz, int = 5). As with complexes **1** and **2**, the $^{31}$P NMR spectrum is indicative of fluxional behavior.

The $^{13}$C NMR solution spectrum ($CDCl_3$, 25 °C) of the $^{13}$CO analogue of **3**, as shown in Figure 6, consisted of a sextet of doublets at $\delta$ 208.4 ($^2J_{^{13}C-P}$ = 3.0 Hz, $^3J_{^{13}C-P}$ = 13.2 Hz) with $^{195}$Pt satellites ($J_{^{195}Pt-^{13}C}$ = 1330 Hz). The IR spectrum (KBr) of **3** displayed a $\nu$(CO) absorption at 1946 cm$^{-1}$, which is consistent with a terminal bound metal carbonyl. The absorption shifted to lower energy (1900 cm$^{-1}$) when **3** was synthesized with 99% $^{13}$CO.

Positive-ion FABMS analysis yielded a spectrum with well-resolved peaks. In agreement with the formulation of **3** as $[(PPh_3)(CO)Pt(AuPPh_3)_5]^+$, the conductance of **3** in $CH_3CN$ showed it to be a 1:1 electrolyte, whether the counterion was $Cl^-$, $NO_3^-$, or $PF_6^-$.

The CO stretching vibrations in the IR spectra for complexes **2** and **3** (1967 and 1946 cm$^{-1}$, respectively) are indicative of a carbonyl ligand terminally bound to a transition metal. The corresponding values (1923 and 1900 cm$^{-1}$, respectively) obtained for the $^{13}$CO-labeled compexes are in excellent agreement with the energies theoretically calculated by using Hooke's law. In removal of a $Au(PPh_3)$ moiety from complex **2** to form complex **3**, the formal charge of the cluster decreases from +2 to +1. This is evidenced by the decrease in energy of the $\nu$(CO) absorption and reflects an increased $\pi$-back-bonding interaction due to more electron density on the Pt atom. This same result is observed in the complexes $[(CO)(Ag)Pt(AuPPh_3)_8]^{3+}$ and $[(CO)Pt(AuPPh_3)_8]^{2+}$, in which the $\nu$(CO) absorption is at 1964 and 1940 cm$^{-1}$, respectively.[58]

The chemical shifts of the carbonyl carbons in the $^{13}$C NMR spectra of complexes **2** and **3** ($\delta$ 208.2 and 208.4, respectively) are found substantially downfield from the chemical shifts in monomeric carbonyl-substituted Pt complexes ($\delta$ 149–182)[59] but are similar to the value reported for $[(CO)Pt(AuPPh_3)_8]^{2+}$ ($\delta$ 210.7).[7] These downfield chemical shifts found for complexes **2** and **3** suggest that the formal charge on the Pt atom is very low or possibly even slightly negative. The low values of the CO stretching frequencies for complexes **3** and $[(CO)Pt(AuPPh_3)_8]^{2+}$ (1940 cm$^{-1}$) are especially suggestive of this.[7]

**Acknowledgment.** This work was supported by the National Science Foundation and the donors of the Petroleum Research Fund, administered by the American Chemical Society.

**Supplementary Material Available:** Figures S1 and S2, displaying the ORTEP drawings of **1** and **2**, Table S1, listing complete crystal data and data collection parameters, and Tables S2–S11, listing general temperature factor expressions, final positional and thermal parameters for all atoms including solvate molecules, distances, angles, and least-squares planes (42 pages); Tables S12 and S13, listing observed and calculated structure factor amplitudes (95 pages). Ordering information is given on any current masthead page.

---

(57) Robertson, G. B.; Tucker, P. A.; Wickramasinghe, W. A. *Aust. J. Chem.* **1986**, *39*, 1495.

(58) Kanters, R. P. F.; Schlebos, P. P. J.; Bour, J. J.; Bosman, W. P.; Smits, J. M. M.; Beurskens, P. T.; Steggerda, J. J. *Inorg. Chem.*, submitted for publication.

(59) Mann, B. E.; Taylor, B. F. In *$^{13}$C NMR Data for Organometallic Compounds*; Maitlis, P. M.; Stone, F. G. A., West, R., Eds.; Academic Press: London, 1981; p 181.